Nigerian Journal of Physics (NJP)
ISSN online: 3027-0936
ISSN print: 1595-0611
DOI: https://doi.org/10.62292/njp.v33(s).2024.219
Volume 33(S) 2024

Growth rate of AL_2O_3 Thin Film by Liquid Phase Deposition as an Anti-reflection Coating Layer on Crystalline Silicon for Solar Cell Applications

***[1]Suleman, K. O., [2]Abdul-Azeez, H., [1]Ezike, F. I., [1]Oyor, D. I., [1]Nwauzor, J. N., [1]Kalu, J., [3]Alor, K. P., [4]Ugbaja, C. M., [4]Okereke, B. O. and [4]Nwaneho, F. U.**

[1]Department of Science Laboratory Technology, Akanu Ibiam Federal Polytechnic, Unwana, Afikpo, Ebonyi State. Nigeria.
[2]Department of Physics, Adamawa State College of Education, Hong, Nigeria.
[3]Department of Physics and Industrial Physics, Nnamdi Azikiwe University, Awka, Anambra State. Nigeria.
[4]Department of Physics, Federal University of Technology, Owerri. Imo State. Nigeria.

[*]Corresponding author's email: kosuleman@akanuibiampoly.edu.ng Phone: +2347068508743

ABSTRACT
The fabrication of photovoltaic (PV) device requires that surface reflectance of solar cells has to be minimized to achieve higher photo-conversion efficiency (PCE). Antireflection coating layer is deposited on the surface of a p-type crystalline silicon material to reduce the surface reflections of solar radiation and increase its absorption for efficient solar cell application. In this work, aluminum oxide thin film by liquid phase deposition (LPD-Al_2O_3) is synthesized from combined solution of aluminum sulfate octadecahydrate ($Al_2(SO_4)_3 \cdot 18H_2O$) and sodium carbonate ($NaHCO_3$) with pH of 3.1. Some samples of p-type (100) crystalline silicon (c-Si) wafers of resistivity 1 – 10 mΩ were immersed inside the growth liquid of LPD-Al_2O_3 thin film for 1hr – 2.5 hours. This is followed by annealing the samples at a temperature of 450°C, the deposition rate is faster in the range 1 – 1.5 hours is about 35nm/hr. As the growth time increases, the growth rate of the film decreases and remains nearly constant at about 10 nm/hour at 1 – 2 hours. When the growth time exceeds 2 hours, the film thickness remains unchanged showing that the liquid has lost in growth ability. The weighted average reflection (R_{avg} %) of planar c-Si is reduced from 44.9 % to 29.6 % after deposition of the LPD-Al_2O_3 for 2.5 hours growth time, indicating a 34.1 % reduction in reflection within wavelength region of 300–1100 nm. While the root means square (RMS) surface roughness of 36.5 nm was also recorded at the highest growth time of 2.5 hours. This shows the effect of thicker LPD-Al_2O_3 thin film layer increases the anti-reflecting coating property of the material.

Keywords:
Aluminum oxide thin film,
Weighted average reflection,
RMS surface roughness,
Anti-reflecting coating.

INTRODUCTION

Solar energy has emerged as a global alternative energy source in recent years due to its abundance, accessibility, environmental friendliness, and renewable nature. This energy has been harnessed using modern technologies (Lin et al., 2016). It lessens the impact of global warming, in contrast to certain other energy sources. Photovoltaic (PV) cells are among the most widely used semiconductor technologies for converting thermal energy from solar radiation into electrical energy or electricity. Crystalline silicon (c-Si) is the most utilized semiconductor material in the photovoltaic manufacturing business. This is because it is a plentiful element that can be found both on and below the surface of the Earth, and it has the capacity to absorb solar energy (Jia et al., 2017; Özkol et al., 2020). In the 300–1100 nm wavelength range, it still has an average reflectance rate of roughly 35% despite its noticeable degree of broadband light absorption (Wang et al., 2021). A variety of ARC materials are available, such as organic ARC layer (Chai et al., 2020), metamaterials ARC (Fan et al., 2021), dielectric ARC material (Viswanath, 2001), and multilayered ARC structures (Barreda et al., 2019). In order to increase solar cell efficiency, ARC is required to decrease reflection losses that occur at the Si-air contact. This is accomplished by maximizing light absorption in the semiconductor material's active layer, which raises the efficiency of solar cell conversion. Light emitting diodes (LEDs), integrated circuits, solar cells, photosensors, transistors,

and other semiconductor devices are among the devices that use it (Hou et al., 2021). Silicon dioxide (SiO_2), silicon nitride (Si_3N_4), and aluminum oxide (Al_2O_3) are the most frequently reported ARC materials that suppress reflection in b-Si (Özkol et al., 2020). High temperatures are needed to create SiO_2, which makes the process costly. Additionally, the inherited positive fixed charges of SiO_2 or SiNx might induce poor passivation for p-type silicon surfaces due to the resultant depletion that increases the likelihood of minority carriers recombining (Lee et al., 2018).

Because of its chemical and field effect capabilities, Al_2O_3 is now thought to be an excellent ARC material (Castillo et al., 2017; Balaji et al., 2020). With its high refractive index (~1.6) at 600 nm, wide band gap (Eg ~ 9 eV), good thermal conductivity, great transparency in the ultraviolet and visible spectra throughout a wavelength range of 200 – 800 nm, and good electrical insulation, Al_2O_3 is a promising resource (Dingemans and Kessels, 2012; Hsu et al., 2019). Al_2O_3 has many uses, such as in transparent ceramics (Singh et al., 2018), integrated circuit baseboards (Angarita et al., 2017), cosmetic fillers (Li et al., 2020), polishing materials (Ding et al., 2017), and others. In terms of radiation resistance and impurity inhibition, including sodium ions, it outperforms SiO_2 and Si_3N_4 (Chen et al., 2021). It is more resilient to basic corrosion and a variety of acids than SiO_2. Hence, it is utilized in semiconductor electrical devices as an enhanced dielectric as an ARC layer (Lin et al., 2016).

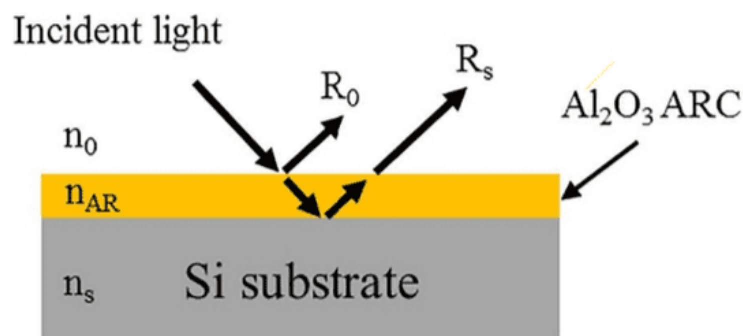

Figure 1: Conventional diagram of antireflection coating of Al_2O_3/Si (Lin et al., 2016)

The primary techniques described in the literature for preparing Al_2O_3 thin films on semiconductor material include electron beam evaporation (Nabhan et al., 2023), magnetron sputtering (Yan et al., 2013), atomic layer deposition (ALD) (Fukushima et al., 1994; Hannebauer et al., 2015; Musil et al., 2010), and plasma-enhanced chemical vapour deposition (PECVD) (Getz et al., 2021). While Al_2O_3 films made with these methods are usually of great quality, they necessitate extremely high temperatures and costly equipment. As a result, we provide LPD-Al_2O_3, or liquid phase deposition, as a straightforward, inexpensive, large-area coverage thin film, and non-toxic technique for depositing Al_2O_3 (Ghiraldelli et al., 2008). Zhang et al. report that to examine the impact of annealing temperature on the optical and structural properties, an Al_2O_3 thin film with a thickness of approximately 80 nm was formed as an ARC layer on p-type b-Si using the chemical liquid phase deposition technique (CLD) (Zhang et al., 2017). Al_2O_3 ARC was also deposited via RF sputtering and annealing on p-type Si wafers. As a result, the Al_2O_3's refractive index increased from 1.69 to 1.74 with an annealing temperature of 300 to 600°C. The annealing temperature also induced a rise in coat density because it rearranges the Al_2O_3 atoms (Repo et al., 2011). Al_2O_3 film of thickness 40nm is deposited on Si nanowires on c-Si, SiNWs/Si as both ARCs and passivation layer using LPD to decrease reflectivity of 1.57 % to 0.98 %, improving absorption by ~63 % (Jia et al., 2017)

In this work, four samples of p-type (100) c-Si are immersed in a growth liquid of LPD-Al_2O_3 thin film of pH 3.1 as an ARC layer by dip coating method from 1 hour to 2.5 hours and annealed at 400°C for 1 hour. The optical and morphological properties of the substrates are characterized and the relationship between R_{avg} and potential short circuit current $J_{sc(max)}$ is used to determine the reflectivity performance of LPD-Al_2O_3 ARC layer on Si within the wavelength 300 – 1100 nm. The values of $J_{sc(max)}$ enhancement is generated from the expected results for each substrate. The research also shows that as growth time of the LPD-Al_2O_3 thin film increases, the R_{avg} on the surface of the c-Si decreases and potential $J_{sc(max)}$ increases for improving solar cell efficiency.

MATERIALS AND METHODS

RCA cleaning of c-Si

In this research, p-type monocrystalline silicon (c-Si) wafer <100> of 250 µm thickness and a resistivity of 1–10 Ωcm is used. The standard Radio Corporation of

America (RCA) technique is used to clean the c-Si. A mixture of 50ml of deionized water (DI H_2O), 10ml of hydrogen peroxide H_2O_2 and 10ml of ammonium hydroxide NH_3OH in the ratio $5H_2O{:}1H_2O_2{:}1NH_3OH$ in a glass beaker is heated until 75°C. the samples of the p-type c-Si are immersed in the heated solution and maintained at 80°C for 10 minutes. The samples are rinsed in DI H_2O and then immersed in a solution of 50 ml of DI H_2O and 1ml of hydrofluoric acid HF ($50H_2O{:}1HF$) for 10 – 15 sec. each to make them hydrophobic. These samples are then immersed in another solution of 60ml of deionized water (DI H_2O), 10 ml of hydrogen peroxide H_2O_2 and 10 ml of hydrochloric acid HCl in the ratio $6H_2O{:}1H_2O_2{:}1HCl$ in a glass beaker and then heated until 75°C. The samples are heated for another 10 minutes and then transferred into a beaker of DI H_2O for few minutes before drying with nitrogen gas N_2.

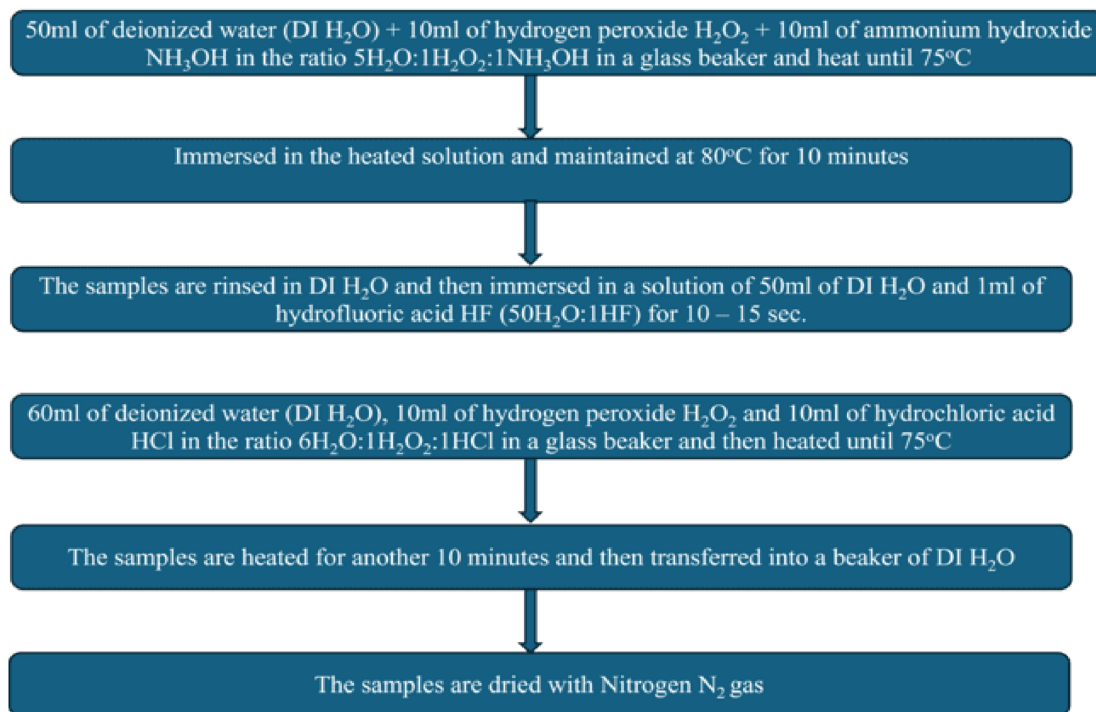

Figure 2: Diagrammatic Process of RCA cleaning of c-Si

Synthesizing of LPD-Al_2O_3 thin film

Sodium carbonate ($NaHCO_3$) and aluminum sulfate octadecahydrate $Al_2(SO4)_3{\cdot}18H_2O$ are the precursor chemicals needed to manufacture LPD- Al_2O_3 thin film. In a Teflon beaker, dissolve 50g of $Al_2(SO4)_3{\cdot}18H_2O$ in 50 ml of DI H_2O at room temperature and mix well. A slightly viscous translucent liquid with a pH of 2.86 is obtained by filtering away the undissolved particles using filter paper. A magnetic stirrer is used to mix the $Al_2(SO4)_3{\cdot}18H_2O$ solution once it has been transferred into a different beaker. Before adding further powder, slowly add 13.5 g of $NaHCO_3$ powder to the solution until the foamy CO_2 goes away. The particles were completely dissolved using an ultrasonic instrument, yielding a transparent, colorless, viscous solution with a pH of around 2.91. Filter sheets measuring 5 µm were used to filter the mixture. To prevent the long-term production of aluminum sodium vanadium, this combination was diluted right away with 150 milliliters of DI water. The growing fluids had a pH of roughly 3.1. The reaction as it appears in equations (1) and (2) is shown below.

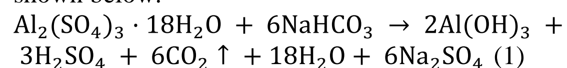

$$Al_2(SO_4)_3\cdot 18H_2O + 6NaHCO_3 \rightarrow 2Al(OH)_3 + 3H_2SO_4 + 6CO_2\uparrow + 18H_2O + 6Na_2SO_4 \quad (1)$$

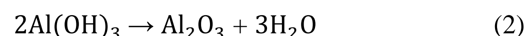

$$2Al(OH)_3 \rightarrow Al_2O_3 + 3H_2O \quad (2)$$

The four samples of c-Si substrates were immersed into the thin film of Al_2O_3 produced through the LPD technique (LPD-Al_2O_3) for 1, 1.5, 2 and 2.5 hours each. The growth liquid was deposited, rinsed with DI water, and then dried with a N_2 atmosphere. The substrates were annealed in a furnace at a temperature of 400°C for 1 hour in an ambient N_2 environment to ensure proper adhesion, increase the density of thin film and efficient passivation property. This step can also eliminate the possible existence of hydrogen element although negligible.

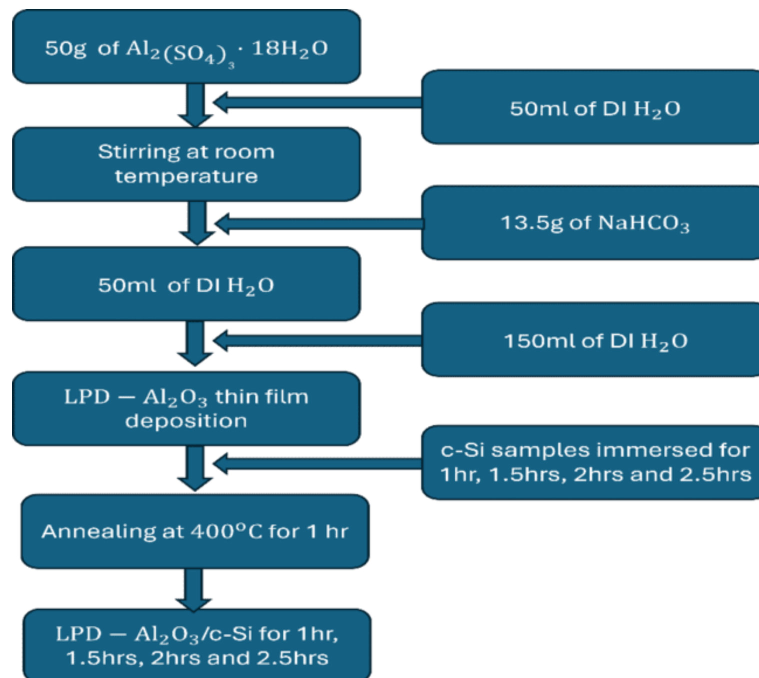

Figure 3: Diagrammatic preparation of LPD-Al_2O_3 thin film

Samples Characterization and Measurement

Using field emission scanning electron spectroscopy (FESEM; Model: FEI Nova NanoSEM 450), the thickness and surface morphology of the LPD-Al_2O_3 thin film, which has a mirror-like surface, are characterized on the substrates. The atomic force microscope (AFM; Model: Dimension Edge, Bunker) was used to measure the height and root means square (RMS) surface roughness of the substrates over a scan range of $10 \times 10\ \mu m^2$. Using an integrating sphere (Model: Agilent Cary 500) and a UV-vis-NIR spectrophotometer, the optical characteristics of the substrate were measured between 300 and 1100 nm. The LPD-Al_2O_3 thin film deposit thickness was examined using the Image J computer application program. By integrating the product of absolute reflectance R(λ) and the spectral photon density under standard AM 1.5G solar spectrum S(λ) within the wideband of 300 – 1100 nm, equation (1) was utilized to calculate the weighted average reflection (R_{avg} %) of the substrates, as illustrated below (Song et al., 2013).

$$R_{avg} = \frac{\int_{\lambda=300nm}^{\lambda=1100nm} R(\lambda)S(\lambda)d\lambda}{\int_{300nm}^{1100nm} S(\lambda)d\lambda} \qquad (3)$$

where R(λ) represents absolute reflectance, S(λ) represents spectral photon density under standard AM 1.5G solar spectrum and λ represents the wavelength of light. The absorption (A) of light through the samples can be obtained from the equation $A = (100 - R - T)\%$ (Özkol et al., 2020). From the equation, the transmission (T) is zero because the c-Si is an opaque body, which cannot allow light to transmit through it. Therefore, the equation becomes $A = (100 - R)\%$. The result from the absorption, the light-coupling performance of the LPD-Al_2O_3 on the samples can be achieved using the potential $J_{sc(max)}$. The equation (4) below can be used to calculate the value of potential $J_{sc(max)}$ for the wavelength region of 300 – 1100 nm (Wang et al., 2021).

$$J_{sc(max)} = q\int_{\lambda=300nm}^{\lambda=1100nm} EQE(\lambda).S(\lambda)d\lambda \qquad (4)$$

RESULTS AND DISCUSSION

Morphological characterization

Figure: 4 (a) – (e) describes the images from AFM tilted at 45° of c-Si, LPD-Al_2O_3/c-Si 1hr, LPD-Al_2O_3/c-Si 1.5 hours, LPD-Al_2O_3/c-Si 2 hours and LPD-Al_2O_3/c-Si 2.5 hours respectively. From the images displayed by the AFM, it can be deduced that the RMS surface roughness increases with the growth rate and is affected by the annealing temperature of 400°C for 1 hour in the blue furnace. The root mean square (RMS) roughness of pure c-Si is 2.18 nm, the LPD-Al_2O_3/c-Si deposition for 1 hour is 26.7 nm while deposition for 1.5 hours is 27.2 nm. Also, the RMS surface roughness for deposition of 2 hours is 36.5 nm and that of 2.5 hours is 29.8 nm. This indicates that at deposition of LPD-Al_2O_3 on c-Si reaches its optimal growth limit at 2 hours and remain constant until 2.5 hours.

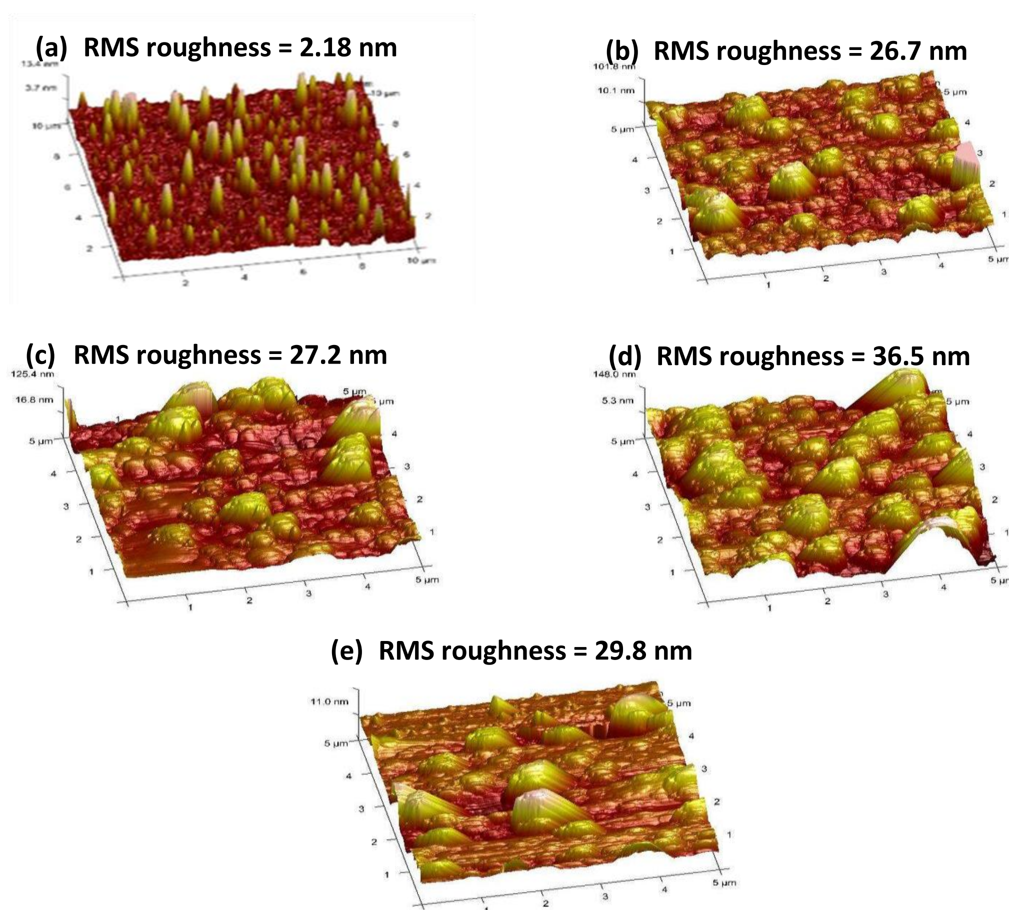

Figure 4: AFM images of (a) planar c-Si (b) LPD-Al_2O_3/c-Si 1hour (c) LPD-Al_2O_3/c-Si 1.5 hours (d) LPD-Al_2O_3/c-Si 2 hours (e) LPD-Al_2O_3/c-Si 2.5 hours deposition time and annealed at 400°C for 1 hour

Also Figure 5: (a and b) illustrates the FESEM results showing the top view of the c-Si and LPD-Al_2O_3/c-Si substrates. The top view (10,000 magnification) of the planar c-Si shows no sign of deposition as seen in Figure 5(a). Proper observation on the top view FESEM image of LPD-Al_2O_3/c-Si in figure 5(b) shows a uniformly and continuous spread of LPD-Al_2O_3 thin film with few bumps. Generally, a smooth insulating layer of the thin film is preferable because of the good interface contact with the c-Si wafer, which can improve the stability and electrical performance of the solar cell. The cross-sectional FESEM image of LPD-Al_2O_3/c-Si in Figure 5(c) shows a smooth layer of the thin film deposited which thickness is 30 nm. This thickness corresponds to [5].

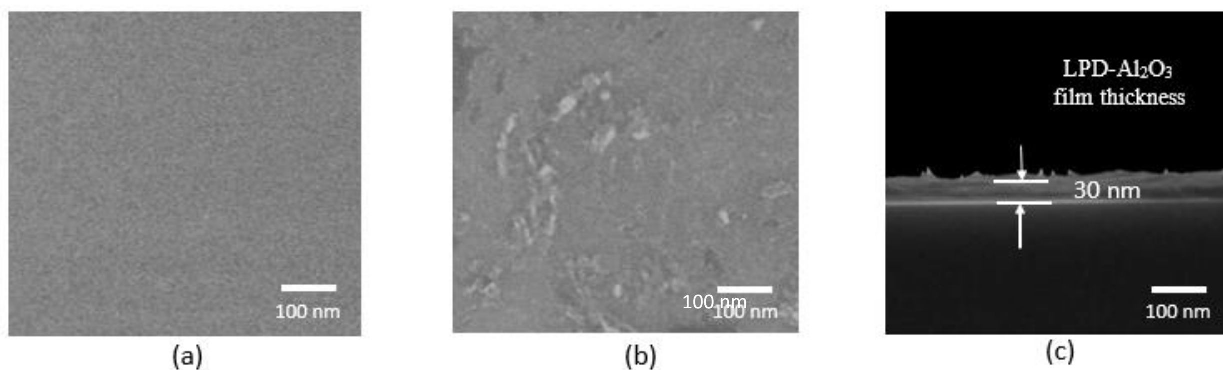

Figure 5: Top view of (a) pure c-Si (b) LPD-Al_2O_3/c-Si and (c) cross-sectional view of LPD-Al_2O_3/c-Si showing a thickness of 30 nm thin film

Figure 6: Explains the EDX spectrum of the LPD-Al_2O_3 thin film deposited Si substrate with a scan range of 0 to 10 keV, 400°C annealing temperature. The figure shows that the apparent signals of Al and O are located at 1.50 and 0.50 keV, respectively. There are no other peaks found, indicating that the LPD-Al_2O_3 thin film chemical composition process is impurity-free. This is in addition to the Si peak. The atomic ratio of the O element to the Al element is estimated to be roughly 7:3, which deviates from the predicted 3:2 ratio based on the peak values found. Because of the excess oxygen in the thin film, the presence of LPD-Al_2O_3 results in a negative fixed charge Q_f between the LPD-Al_2O_3/c-Si interface. This suggests that the LPD-Al_2O_3 thin film has a low thickness. This supports reference (Cibert et al., 2008).

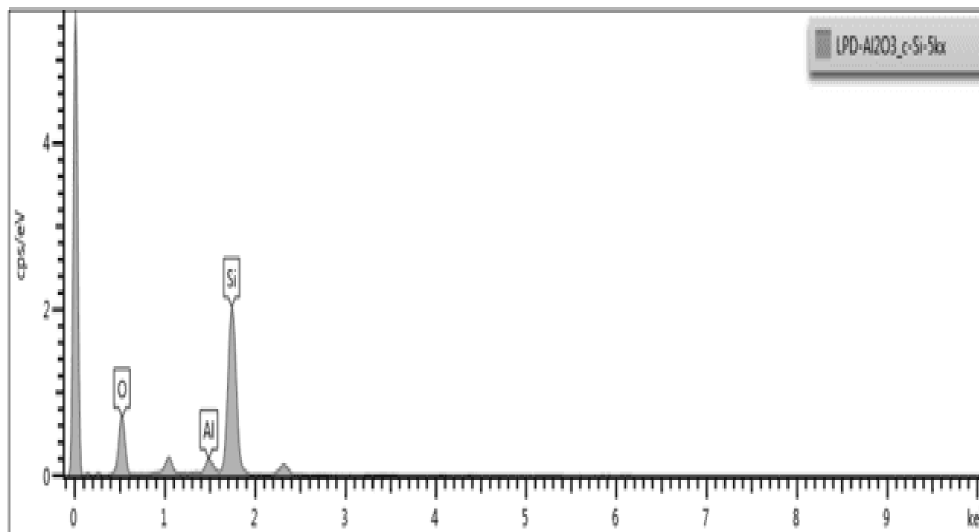

Figure 6: EDX spectra analysis of LPD-Al_2O_3 thin film on silicon after annealing at 400ºC for 1 hr

Optical characterization

Figures 7: (a) and (b) show the total reflection and absorption of all the substrates from the UV-vis-NIR characterization. The equation (3) above is used to calculate R_{avg} of total reflection obtained from the curve within the wavelength 300 – 1100 nm region. The c-Si and LPD-Al_2O_3/c-Si of several growth film deposition time samples are compared. The R_{avg} of the c-Si at a wavelength of 600 nm is 44.9% while the R_{avg} of LPD-Al_2O_3/c-Si 1hr is 35.0 %. Also, the R_{avg} of LPD-Al_2O_3/c-Si 1.5 hours deposition is 35.3 % while that of LPD-Al_2O_3/c-Si 2 hours is 34.7 %. lastly, the R_{avg} of LPD-Al_2O_3/c-Si 2.5 hours is 29.6 %. The trends show that the increase in growth time of the thin film on the substrates causes a reduction in reflection of the c-Si. Hence, improve absorption of light energy for better efficiency and performance of solar cell applications. The percentage reduction or improvement in reflectivity is calculated with the equation $\left[\left(Abs\frac{(b-a)}{b}\right)100\%\right]$, where b and a are the weighted average reflectance of substrates before and after the deposition of the LPD-Al_2O_3 film respectively.

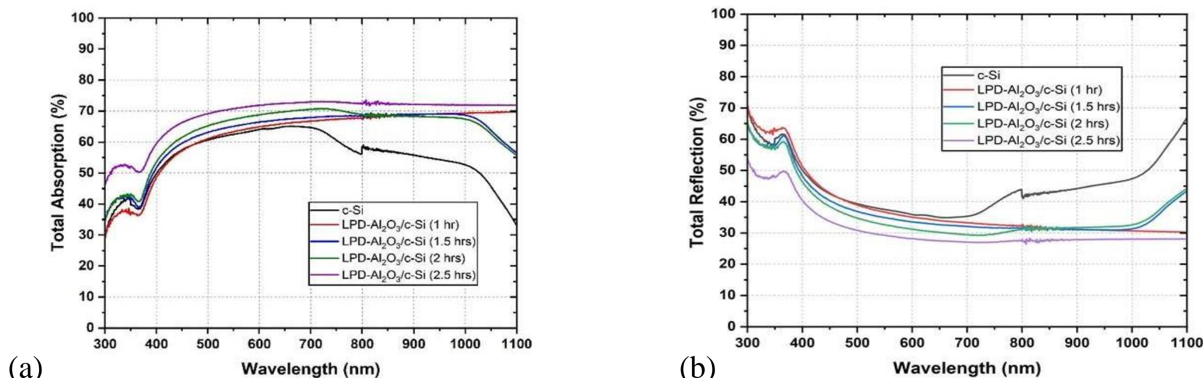

Figure 7: (a) Total reflection and (b) Total absorption curves of all samples annealed at 400ºC for 1 hour

Figure 8: exhibits the XRD patterns of LPD-Al_2O_3 films deposited on c-Si and annealed at 400 °C for 1 hr. It can be seen that after the LPD-Al_2O_3 film is annealed at 400 °C, only the diffraction peaks $\alpha -Al_2O_3$ (220) located at 89.9°C is observed. This makes the emergency of (400) and (440) planes indicate the structure of Al_2O_3 becomes γ-Al_2O_3. It means the film can crystallize to be γ-Al_2O_3 at a relatively low temperature. Although, no other peak corresponding to the $\alpha -Al_2O_3$ (220) was observed, suggesting amorphous γ-Al_2O_3 thin films were obtained almost over the entire range of the annealing temperature. The amorphous nature of γ-Al_2O_3 dielectric is preferable because grain boundaries in poly-crystalline structure act as preferential paths for impurity diffusion and leakage currents, and certainly cause an inferior dielectric reliability (Zhang et al., 2017).

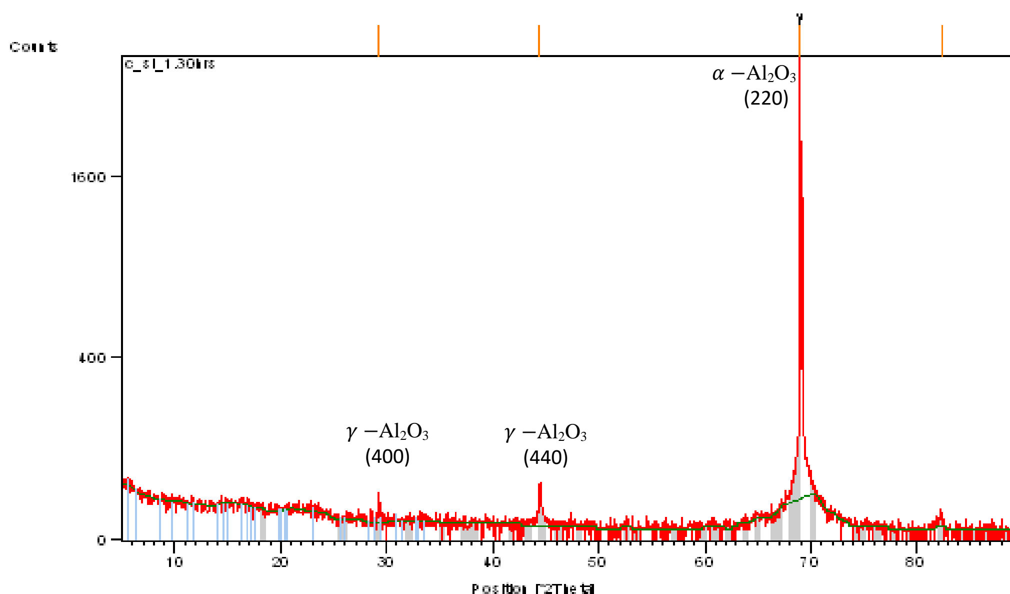

Figure 8: XRD patterns of LPD-Al_2O_3 films deposited on c-Si and annealed at 400 °C for 1 hour

The Table 1 below show the relationship between the potential $J_{sc(max)}$ and R_{avg} of the samples immersed in the growth film for different depostion time ranging from 1 – 2.5 hours and the pure c-Si, after annealing at 400°C for 1 hour. The Equation (4) above is used to achieve the potential $J_{sc(max)}$ and potential $J_{sc(max)}$ enhancement (%) by comparing the improvement of the other samples to the planar c-Si which represents the reference sample with R_{avg} of 44.9 % and potential $J_{sc(max)}$of 22.5 mA/cm^2. The LPD-Al_2O_3/c-Si 1hour sample with R_{avg} 35.0 %, has an increased potential $J_{sc(max)}$value of 23.8 mA/cm^2 and an enhancement of 5.8 % because of low light reflection within a wavelength of 300 – 1100 nm. Also, the LPD-Al_2O_3/c-Si 1.5 hours and LPD-Al_2O_3/c-Si 2 hours sample of R_{avg} are 35.3 % and 34.7 % exhibit a potential $J_{sc(max)}$ of 23.4 mA/cm^2 and 24.7 mA/cm^2 with an enhancement of 4.0% and 9.8% respectively compared to pure c-Si. Finally, LPD-Al_2O_3/c-Si 2.5 hours with the lowest R_{avg} of 29.6 %, has potential $J_{sc(max)}$ and potential $J_{sc(max)}$ enhancement of 27.2 mA/cm^2 and 20.9 % respectively. This can be attributed to the improved broadband light absorption by the LPD-Al_2O_3 roughness on the surface of the planar c-Si wafer.

Table 1: Relationship between R_{avg} and potential $J_{sc(max)}$for all the samples.

Sample	R_{avg}(%)	Potential $J_{sc(max)}$(mA/cm^2)	Potential $J_{sc(max)}$ enhancement (%)
c-Si	44.9	22.5	-
LPD-Al_2O_3/c-Si 1 hour	35.3	23.8	5.8
LPD-Al_2O_3/c-Si 1.5 hours	35.0	23.4	4.0
LPD-Al_2O_3/c-Si 2 hours	34.7	24.7	9.8
LPD-Al_2O_3/c-Si 2.5 hours	29.6	27.2	20.9

CONCLUSION

In this work, the growth rate of LPD-Al_2O_3 thin film deposition on c-Si was studied. The LPD-Al_2O_3 thin film was prepare from precursor chemicals mixtures of $Al_2(SO_4)_3 \cdot 18H_2O$ and $NaHCO_3$ dissolved in DI H_2O at room temperature and obtain a pH of 3.1. Four samples of c-Si were immersed in the LPD-Al_2O_3 thin film for 1, 1.5, 2 and 2.5 hours and annealed in the furnace at a temperature of 400ºC for an hour in N_2 ambient. From the UV-vis curve, the R_{avg} of the samples including planar c-Si, LPD-Al_2O_3/c-Si 1hr, LPD-Al_2O_3/c-Si 1.5 hours, LPD-Al_2O_3/c-Si 2 hours and LPD-Al_2O_3/c-Si 2.5 hours are 44.9 %, 35.3 %, 35.0 %, 34.7 % and 29.6 % respectively. Also, the values absorption is 55.1 %, 64.7 %, 65.0 %, 65.3 % and 70.4 % respectively. The AFM images show RMS surface roughness of each sample. The reference sample (planar c-Si) has a smooth RMS surface roughness of 2.18 nm because no deposition of LPD-Al_2O_3 on its surface. The RMS surface roughness increased because of growth rate of LPD-Al_2O_3 thin film and annealing at 400ºC for 1 hour. The RMS surface roughness of LPD-Al_2O_3/c-Si at 1, 1.5, 2 and 2.5 hours are 26.7 nm, 27.2 nm, 36.5 and 29.8 nm respectively. Moreso, the potential $J_{sc(max)}$ of the planar c-Si without any deposition is 22.5 mA/cm^2, while LPD-Al_2O_3/c-Si 2.5 hours has a potential $J_{sc(max)}$ of 27.2 mA/cm^2 resulting in $J_{sc(max)}$ enhancement by 20.9 % compared to the reference substrate (planar c-Si). It can be deduced that the deposition of LPD-Al_2O_3 thin film on b-Si substrate followed by annealing at a temperature of 500ºC for 1 hour, decreases R_{avg}, increases the RMS surface roughness and increases the potential $J_{sc(max)}$ of the substrate.

REFERENCES

Angarita, G., Palacio, C., Trujillo, M., & Arroyave, M. (2017). Synthesis of Alumina Thin Films Using Reactive Magnetron Sputtering Method. Journal of Physics: Conference Series, 850(1). https://doi.org/10.1088/1742-6596/850/1/012022

Balaji, P., Dauksher, W. J., Bowden, S. G., & Augusto, A. (2020). Improving surface passivation on very thin substrates for high efficiency silicon heterojunction solar cells. Solar Energy Materials and Solar Cells, 216. https://doi.org/10.1016/j.solmat.2020.110715

Barreda, A. I., Saiz, J. M., González, F., Moreno, F., & Albella, P. (2019). Recent advances in high refractive index dielectric nanoantennas: Basics and applications. In *AIP Advances* 9(4). American Institute of Physics Inc. https://doi.org/10.1063/1.5087402

Castillo, M. L., Ugur, A., Sojoudi, H., Nakamura, N., Liu, Z., Lin, F., Brandt, R. E., Buonassisi, T., Reeja-Jayan, B., & Gleason, K. K. (2017). Organic passivation of silicon through multifunctional polymeric interfaces. Solar Energy Materials and Solar Cells, 160, 470–475. https://doi.org/10.1016/j.solmat.2016.10.050

Chai, J. Y. H., Wong, B. T., & Juodkazis, S. (2020). Black-silicon-assisted photovoltaic cells for better conversion efficiencies: a review on recent research and development efforts. In Materials Today Energy, 18, Elsevier Ltd. https://doi.org/10.1016/j.mtener.2020.100539

Chen, H., Shimai, S., Zhao, J., Mao, X., Zhang, J., Zhou, G., & Wang, S. (2021). Highly oriented α- Al_2O_3 transparent ceramics shaped by shear force. Journal of the European Ceramic Society, 41(6), 3838–3843. https://doi.org/10.1016/j.jeurceramsoc.2021.01.014

Cibert, C., Hidalgo, H., Champeaux, C., Tristant, P., Tixier, C., Desmaison, J., & Catherinot, A. (2008). Properties of aluminum oxide thin films deposited by pulsed laser deposition and plasma enhanced chemical vapor deposition. Thin Solid Films, 516(6), 1290–1296. https://doi.org/10.1016/j.tsf.2007.05.064

Ding, S. J., Huang, Y. J., Huang, Y., Pan, S. H., Zhang, W., & Wang, L. K. (2007). High density Al_2O_3 /TaN-based metal-insulator-metal capacitors in application to radio frequency integrated circuits. Chinese Physics, 16(9), 2803–2808. https://doi.org/10.1088/1009-1963/16/9/051

Dingemans, G., & Kessels, W. M. M. (2012). Status and prospects of Al_2O_3-based surface passivation schemes for silicon solar cells. Journal of Vacuum Science & Technology A: Vacuum, Surfaces, and Films, 30(4), 040802. https://doi.org/10.1116/1.4728205

Fan, Z., Cui, D., Zhang, Z., Zhao, Z., Chen, H., Fan, Y., Li, P., Zhang, Z., Xue, C., & Yan, S. (2021). Recent progress of black silicon: From fabrications to applications. In Nanomaterials, 11(1), 1–26. MDPI AG. https://doi.org/10.3390/nano11010041

Fukushima, Y., Saraie, J., Tabayashi, K., & Shobatake, K. (1994). Photo-CVD of Al_2O_3 thin films using a D 2 lamp.

Getz, M. N., Povoli, M., & Monakhov, E. (2021). Improving ALD-Al_2O_3 Surface Passivation of Si using Native SiO x. https://doi.org/10.21203/rs.3.rs-943524/v1

Ghiraldelli, E., Pelosi, C., Gombia, E., Chiavarotti, G., & Vanzetti, L. (2008). ALD growth, thermal treatments and characterisation of Al_2O_3 layers. Thin Solid Films,

517(1), 434–436. https://doi.org/10.1016/j.tsf.2008.08.052

Hannebauer, H., Schimanke, S., Falcon, T., Altermatt, P. P., & Dullweber, T. (2015). Optimized Stencil Print for Low Ag Paste Consumption and High Conversion Efficiencies. Energy Procedia, 67, 108–115. https://doi.org/10.1016/j.egypro.2015.03.294

Hou, G. J., García, I., & Rey-Stolle, I. (2021). High-low refractive index stacks for broadband antireflection coatings for multijunction solar cells. Solar Energy, 217, 29–39. https://doi.org/10.1016/j.solener.2021.01.060

Hsu, C. H., Cho, Y. S., Wu, W. Y., Lien, S. Y., Zhang, X. Y., Zhu, W. Z., Zhang, S., & Chen, S. Y. (2019). Enhanced Si Passivation and PERC Solar Cell Efficiency by Atomic Layer Deposited Aluminum Oxide with Two-step Post Annealing. Nanoscale Research Letters, 14. https://doi.org/10.1186/s11671-019-2969-z

Jia, X., Zhou, C., & Wang, W. (2017). Optimization of the Surface Structure on Black Silicon for Surface Passivation. Nanoscale Research Letters, 12(1), 193. https://doi.org/10.1186/s11671-017-1910-6

Lee, S. H., Bhopal, M. F., Lee, D. W., & Lee, S. H. (2018). Review of advanced hydrogen passivation for highly efficient crystalline silicon solar cells. Materials Science in Semiconductor Processing, 79, 66–73. https://doi.org/https://doi.org/10.1016/j.mssp.2018.01.019

Li, D., Ruan, L., Sun, J., Wu, C., Yan, Z., Lin, J., & Yan, Q. (2020). Facile growth of aluminum oxide thin film by chemical liquid deposition and its application in devices. Nanotechnology Reviews, 9(1), 876–885. https://doi.org/10.1515/ntrev-2020-0062

Lin, C. C., Huang, J. J., Wuu, D. S., & Chen, C. N. (2016). Surface passivation property of aluminum oxide thin film on silicon substrate by liquid phase deposition. Thin Solid Films, 618, 118–123. https://doi.org/10.1016/j.tsf.2016.04.011

Musil, J., Blažek, J., Zeman, P., Prokšová, Š., Šašek, M., & Čerstvý, R. (2010). Thermal stability of alumina thin films containing γ- Al_2O_3 phase prepared by reactive magnetron sputtering. Applied Surface Science, 257(3), 1058–1062. https://doi.org/10.1016/j.apsusc.2010.07.107

Nabhan, A., Taha, M., & Ghazaly, N. M. (2023). Filler loading effect of Al_2O_3 /TiO_2 nanoparticles on physical and mechanical characteristics of dental base composite (PMMA). Polymer Testing, 117. https://doi.org/10.1016/j.polymertesting.2022.107848

Özkol, E., Procel, P., Zhao, Y., Mazzarella, L., Medlin, R., Šutta, P., Isabella, O., & Zeman, M. (2020). Effective Passivation of Black Silicon Surfaces via Plasma-Enhanced Chemical Vapor Deposition Grown Conformal Hydrogenated Amorphous Silicon Layer. Physica Status Solidi (RRL) – Rapid Research Letters, 14(1), 1900087. https://doi.org/https://doi.org/10.1002/pssr.201900087

Repo, P., Talvitie, H., Li, S., Skarp, J., & Savin, H. (2011). Silicon surface passivation by Al_2O_3: Effect of ALD reactants. Energy Procedia, 8, 681–687. https://doi.org/10.1016/j.egypro.2011.06.201

Singh, P., Jha, R. K., Singh, R. K., & Singh, B. R. (2018). Preparation and characterization of Al_2O_3 film deposited by RF sputtering and plasma enhanced atomic layer deposition. Journal of Vacuum Science & Technology B, Nanotechnology and Microelectronics: Materials, Processing, Measurement, and Phenomena, 36(4). https://doi.org/10.1116/1.5023591

Song, S. Y., Kang, M. G., Song, H.-E., & Chang, H. S. (2013). Improvement on the Passivation Effect of PA-ALD Al_2O_3 Layer Deposited by PA-ALD in Crystalline Silicon Solar Cells. Journal of the Korean Institute of Electrical and Electronic Material Engineers, 26(10), 754–759. https://doi.org/10.4313/jkem.2013.26.10.754

Viswanath, A. K. (2001). Chapter 3 Surface and interfacial recombination in semiconductors.

Wang, S., Wu, X., Ma, F.-J., Payne, D., Abbott, M., & Hoex, B. (2021). Field-Effect Passivation of Undiffused Black Silicon Surfaces. IEEE Journal of Photovoltaics, 11(4), 897–907. https://doi.org/10.1109/JPHOTOV.2021.3069124

Yan, Y., Li, L., See, T. L., Ji, L., & Jiang, Y. (2013). CO_2 laser peeling of Al_2O_3 ceramic and an application for the polishing of laser cut surfaces. Journal of the European Ceramic Society, 33(10), 1893–1905. https://doi.org/10.1016/j.jeurceramsoc.2013.01.023

Zhang, B., Wang, Y., Han, L., Li, Y., & Liu, A. (2017). Controlling of polarity on the surface passivation mechanism of Al_2O_3 for black silicon by CLD. *Journal of Nano Research*, *49*, 18–26. https://doi.org/10.4028/www.scientific.net/JNanoR.49.18